PYROXENE RELATIONS IN A HYPERITE NEAR LYNGDAL, NORWAY

JOHAN J. LAVREAU

Lavreau, J. J.: Pyroxene relations in a hyperite near Lyngdal, Norway. *Norsk Geologisk Tidsskrift,* Vol. 50, pp. 333–340. Oslo 1970.

Pyroxenes from a hyperite body associated with Precambrian gneisses were studied optically, chemically, and by means of X-rays. Pyroxene relations show that crystallization takes place at a temperature higher than the inversion of pigeonite, and proceeds into the stability field of hypersthene. The composition and the mutual relations between the pyroxenes suggest a crystallization process for these minerals.

Johan J. Lavreau, Laboratoire de Minéralogie et Pétrologie, Université Libre de Bruxelles, Brussels, Belgium.

Introduction

The investigated rock is one of the gabbroic bodies which crops out in the surroundings of Lyngdal (extreme South of Norway). It lies 3 km north of the town, northwest of Skoland lake, and is crossed by the E 18 road to Flekkefjord (Fig. 1). It is a well defined and homogeneous crescent-shaped unit, about 1500 m long and 500 m broad. The rock is medium grained (1–2 mm grain size), dark grey in colour, and has a gabbro-dioritic composition (Niggli 1923, p. 126). Some dioritic varieties were also recognized (Table 1). The country rock is a monzonitic phenoblastic gneiss foliated parallel to the elongation of the hyperite body. The contacts are seldom visible, for the area is covered by recent deposits except in its northern part, where the rock is unfortunately tectonized and strongly retrometamorphosed.

Experimental techniques

Plagioclase and pyroxenes were first studied with the aid of the universal stage. After heavy liquid, isodynamic and vibrating plate separation (with final hand-picking), clinopyroxenes were determined by X-rays, using a Guinier quadruple camera (Fe $K\alpha_1$ radiation, Mn filtered, with a quartz monochromator) and determination curves of Zwaan (1954).

Hypersthene was separated and determined in the same way, using a

9 cm Debye-Scherrer camera, with quartz as internal standard. The orientation of the exsolution lamellae was used for their optical identification (Poldervaart & Hess, 1951). X-ray single crystal oscillation photographs were also taken, and determination of the associated phases was made with help of a comparison method (Bown & Gay, 1959).

One rock sample, and the pyroxenes separated from it, were chemically analysed (Table 1).

Pyroxene relations

Three pyroxenes can be seen: hypersthene, diopside and pigeonite. They are mostly clustered, occurring as isolated groups among the plagioclases (Fig. 2). Hypersthene, and more rarely diopside, appear in well developed hypidiomorphic crystals.

The orthopyroxene is unzoned, and weakly pleochroic (pale green to pale brownish red), and contains abundant inclusions of hexagonal shaped hematite (?) flakes, some of which lie parallel to the (100) planes of the host, and exsolution lamellae of diopside disposed parallel to (100).

Small variations in 2 V can be distinguished between the isolated hypersthene crystals and those which are clustered with other pyroxenes; the former have 2V about 56° (± 2°), the latter about 53°. A narrow diopside rim is sometimes present around isolated crystals. The diopsidic lamellae are narrow and rather short ($4\mu \times 50\mu$); they represent less than 5 per cent of the host mineral.

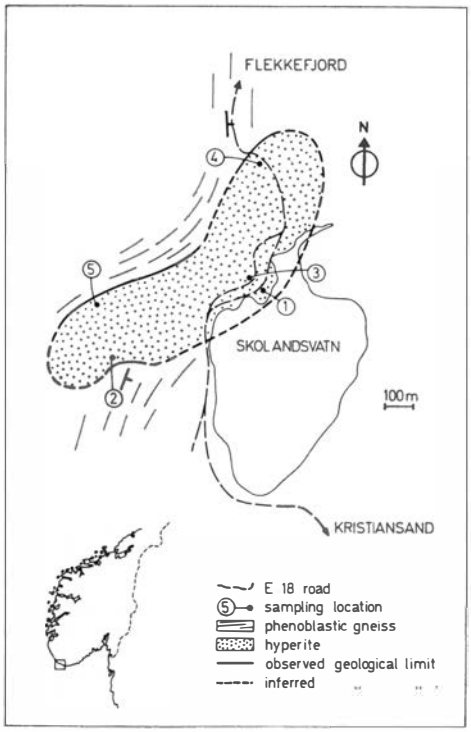

Fig. 1. Map of the hyperite body, and location of sampling points. (1:1/68; 2:2/66; 3:5/66; 4:7/66; 5:17/66).

Table 1

Modal composition of the rock

	Mean	Range	Sample 1/68*	Sample 5/66
Plagioclase	61.15	50.7–67	62.9	50.8
Hypersthene (+ pigeonite)	16.8	13.7–22.3	16.1	22.3
Diopside	5.4	2.4–7.3	5.3	2.5
Biotite	8.0	4.5–11.5	9.1	11.5
Apatite	1.6	0.8–3.0	2.1	1.0
Ore	6.4	4.4–11.8	4.5	11.8

Chemical analyses**

	(1)***	(2)	(3)	(4)		(5)	
SiO_2	49.35	50.50	50.56	1.953	2.000	1.927	2.000
Al_2O_3	17.73	1.61	2.47	0.047		0.073	
				0.026	1.951	0.038	1.980
TiO_2	2.50	1.40	0.60	0.040		0.017	
Fe_2O_3	2.66	1.52	1.81	0.044		0.052	
FeO	6.91	20.50	14.99	0.660		0.476	
MnO	0.13	0.39	0.31	0.012		0.010	
MgO	5.64	17.64	16.38	1.024		0.937	
CaO	7.01	3.16	10.52	0.131		0.430	
Na_2O	3.10	0.19	0.27	0.014		0.020	
K_2O	1.28	–	–				
H_2O	1.85	1.30	0.55				
P_2O_5	0.55	0.09	0.05				
	98.71	98.30	98.51				

(1) total rock 5/66 (wgt. %)
(2) hypersthene 1/68 (wgt. %)
(3) diopside 1/68 (wgt. %)
(4) atomic ratios to 6 0 : hyp. 1/68
(5) di 1/68
* Dioritic variety.
** C. Chaval, analyst.
*** Niggli parameters:

	si	al	fm	c	alk	k	mg	o	qz
this rock:	130	27	43	20	10	.21	.52	.12	11
gabbrodioritic magma type:	135	24.5	42.5	23	10	.28	.50		

Diopside is less abundant, non-pleochroic, xenomorphic in general and zoned (2V varies from 40° to 60° from the centre to the border of the grain). It also contains hematite flakes of the same type as the hypersthene possesses ($2\mu \times 100\mu$). They represent between 5 and 10 per cent of the volume of the host. Some crystals show irregularly shaped lamellae disposed parallel to the (001) planes, thus in a pigeonite orientation. The smallest crystals contain neither hematite nor pyroxene lamellae.

Pigeonite is much less frequent; it resembles hypersthene, and contains the same hematite inclusions and poorly developed exsolution lamellae disposed parallel to (001).

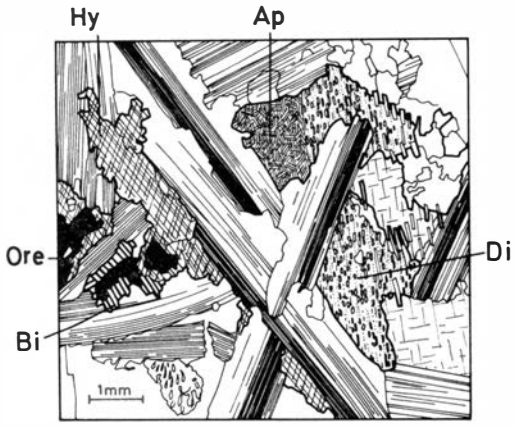

Fig. 2. Micrograph of sample 1/68 showing the ophitic texture, the association of biotite to ore minerals (middle left), the biotite needles growing at the expense of the hypersthene exsolution lamellae (upper and middle right), myrmekite-like micropegmatites bottom left).

The value of 2V and oblique extinction distinguish it from the other pyroxenes. X-ray single crystal examination gave the same identification for the associated phases, and also revealed that the three pyroxenes are present in variable proportions in most of the investigated crystals. Table 2 gives the composition of the pyroxenes deduced from the powder diagrams (see also Fig. 3). The composition of a pigeonite appearing together with hypersthene as foreign lines in a diopside diagram (obtained from a Guinier camera) is also given in spite of some uncertainty as to indexing.

The determination curves of Zwaan (op. cit.) for the clinopyroxenes are limited to the Diopside-Pigeonite-Hedenbergite field, and the composition

Table 2
Composition of pyroxenes

	Sample		Ca	Mg	Fe
X-ray determination	2/66	Di	44.5	50.0	5.5
		Hy	1.3	61.2	37.5
		Pi	5.0	50.0	45.0
	5 and 17/66	Di	40.5	50.0	9.5
		Hy	1.3	64.0	34.7
		Pi	5.0	50.0	45.0
	7/66	Di	44.0	50.0	6.0
		Hy	4.5	59.2	36.3
		Pi	11.5	50.0	38.5
chemical analyse	1/68	Di*	22.6	49.2	28.2
		Hy**	7.0	54.7	38.3

* complete formula:

$(Si, Al)_2O_6\ Ca_{0.43}Mg_{0.94}\ Fe^{2+}_{0.48}\ Mn_{0.01}Al_{0.05}Ti_{0.02}Na_{0.02}Fe^{3+}_{0.05}$

**

$(Si, Al)_2O_6\ Ca_{0.13}Mg_{1.03}\ Fe^{2+}_{0.67}\ Mn_{0.01}Al_{0.04}Ti_{0.04}Na_{0.01}Fe^{3+}_{0.04}$

of pyroxenes having a $Mg_2 Si_2 O_6$ content possibly higher than 50 per cent are plotted on the Di-Pi line. The composition of the orthopyroxene was calculated after assigning half of the Al content to the tetrahedral sites.

Associated minerals

A regularly zoned plagioclase is the most abundant mineral; it occurs in a well-developed ophitic structure, which is locally recrystallized. The composition varies normally from labradorite to oligoclase, but without showing sharply defined zones. Some antiperthitic plagioclase enrichment and abundant micropegmatites (very myrmekite-like) appear in the dioritic variety, together with xenomorphic quartz.

A dark brown biotite is sometimes associated with the pyroxenes, showing a dactilitic structure toward plagioclase (porcupine structure of Sederholm) (Fig. 2). It probably occurs as a result of the retromorphism of the hypersthene lamellae contained in the diopside. The biotite growing into diopside lies with its basal plane parallel to the (100) plane of the host, the mica being elongated and probably oriented along some structural direction of the pyroxene.

Most of the biotite is, however, associated with the ore minerals (Fig. 2). A green hornblende is sometimes present, associated with diopside, occasionally as blebs in hypersthene (probably as result of retromorphism of the diopsidic lamellae).

Opaque minerals, including magnetite, hematite, and sulfides are irregularly distributed in the rock.

Zircon is rare and usually included in biotite.

Apatite crystals are abundant, either as short prisms or as long needles, penetrating the other minerals.

Conditions of crystallization

The coarseness of the exsolution lamellae in the various pyroxenes shows that the cooling of the rock must have been slow, probably in a mesozonal

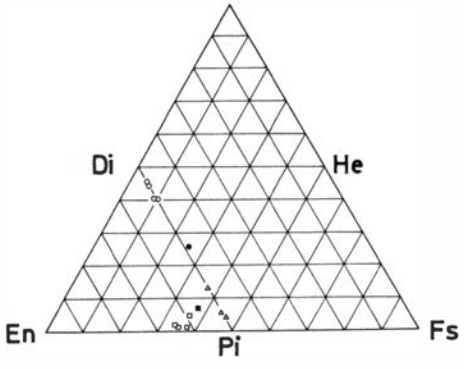

Fig. 3. Composition of the associated pyroxenes (open figures: X-ray determination; solid figures: chemical analyses; circles: diopside; squares; hypersthene; triangles: pigeonite).

environment, as shown by the synantetic minerals. The presence of pigeonite crystals and exsolution lamellae parallel to (001) indicates that the exsolution has taken place at a temperature higher than the pigeonite-hypersthene inversion. Hypersthene crystals, and lamellae parallel to (100), indicate that the crystallization proceeded into the stability field of hypersthene. It is difficult to find out whether pigeonite or hypersthene formed first. If a Mg-hypersthene did (Kuno & Nagashima 1952), it should have undergone a first inversion to pigeonite with falling temperature and variation in composition of the magma accompanying crystallization, and a second one to hypersthene upon further cooling (Fig. 4). There are indeed few chances of finding a trace of a first-formed orthopyroxene after two crossings of the solvus.

Fig. 5 illustrates the presumed crystallization course. Fig. 5b is an approximate Di-En section through the pyroxene field, and takes into account the eventual formation of a Mg-hypersthene. Crystallization thus takes place at subinversion temperatures.

A diopside of composition *i* precipitates together with hypersthene of composition *j*, which on further cooling exsolve respectively a hypersthenic phase *l* and a diopsidic one *k* with a subsequent readjustment of the composition of the host mineral.

Fig. 5a is a Di-Pi section, corresponding to a crystallization beginning at a higher temperature than the hypersthene-pigeonite inversion. A diopside of composition *b* and a pigeonite *c* precipitate from the magma. With decreasing temperature the diopside transforms into a Ca-enriched diopside *d* and a pigeonite *e*. At the same time, the pigeonite *c* transforms into a Ca-poorer pigeonite *e* and a diopside *d*. The transformed phases remain associated as exsolution lamellae.

When the temperature reaches the pigeonite inversion, we have an association of diopside *f* and pigeonite *g*, the latter transforming into an hypersthene *h*. Exsolution proceeds in the crystals as long as temperature allows it.

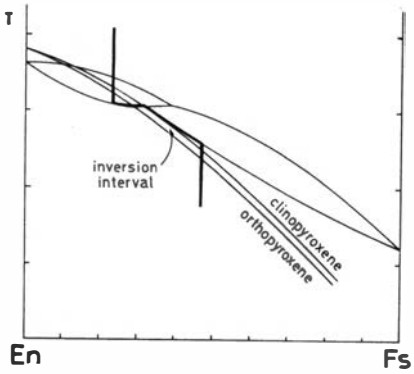

Fig. 4. Liquidus, solidus, and solvus diagram in the system Enstatite-Ferrosilite (adapted from Kuno & Nagashima, 1952). A first formed Mg-rich hypersthene (heavy line) in equilibrium with the magma should invert to pigeonite and again to hypersthene in the course of crystallization and cooling.

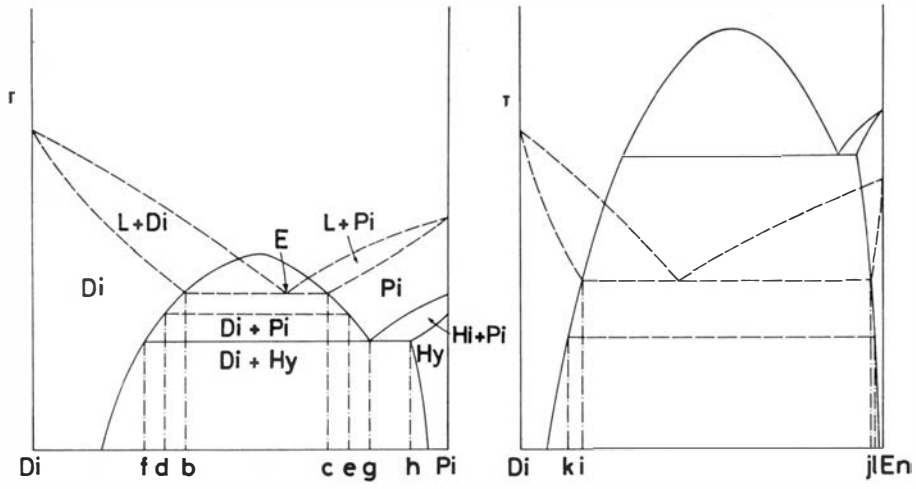

Fig. 5a. Hypothetical liquidus, solidus, and solvus diagram in the system Diopside-pigeonite. The crystallization starts in the stability field of pigeonite (adapted from Muir, 1954, and Barth, 1951).

Fig. 5b. Hypothetical liquidus, solidus, and solvus diagram in the system Diopside-Enstatite. The crystallization starts in the stability field of orthopyroxene.

Chemical relations

The chemical compositions of the pyroxenes are plotted on Figure 3. The composition of the orthopyroxene shows a good agreement with Poldervaart & Hess's (1951) observations on the Mg:Fe ratio in the Ca-poor phase, namely 70:30 in general, extending to 60:40 and 85:15 in some cases. The inaccuracy of the composition determined by X-rays prevents an assessment of the inversion interval (*g–h* in Fig. 5a). Some estimates of the amount of exsolved matter can, however, be made.

By comparing the composition of the analysed pyroxenes and the X-rayed ones, representing respectively the composition of the pyroxenes before and after exsolution, the amount of pyroxene associated as exsolution lamella is 6% of diopside molecule in a hypersthene host, 4% of diopside molecule in a pigeonite host, and 35% of hypersthene molecule in a diopside host.

ACKNOWLEDGEMENTS. The author is indebted to Professor T. F. W. Barth for suggesting the study of some basic rocks in southern Norway and for critically reading an earlier draft of the manuscript. He also wishes to thank colleagues and staff at the Mineralogisk–Geologisk Museum for help in experimental techniques during his stay in Oslo. Chemical analyses were performed in the Laboratories of Mineralogy and Petrology of the Free University of Brussels.

This work was supported by a grant from the 'Accord Culturel Belgo-Norvégien'.

September 1969

REFERENCES

Barth, T. F. W. 1951: Subsolidus diagram of pyroxenes from common mafic magmas. *Norsk Geol. Tidsskr. 29,* 218–221.

Bown, M. G. & Gay, P. 1959: The identification of oriented inclusions in pyroxene crystals. *Amer. Mineral. 44,* 592–602.

Kuno, H. & Nagashima, K. 1952: Chemical composition of hypersthene and diopside in equilibrium in magma. *Amer. Mineral. 37,* 1000–1006.

Muir, I. D. 1954: Crystallization of pyroxenes in an iron-rich diabase from Minnesota. *Min. Mag. 30,* 376–388.

Poldervaart, A. & Hess H. H. 1951: Pyroxenes in the crystallization of basaltic magma. *Jour. Geol. 59,* 472–489.

Niggli, P. 1923: *Gesteins- und Mineralprovinzen Band I: Einführung.* Borntraeger Verlag, Berlin. 602 pp.

Zwaan, P. C. 1954: On the determination of pyroxenes by X-ray powder diagrams. *Leidse Geol. Mededel. 19,* 167–276.